Journal of Oceanology and Limnology
Vol. 39 No. 5, P. 1938-1947, 2021
https://doi.org/10.1007/s00343-020-0215-2

C_{17}-fengycin B, produced by deep-sea-derived *Bacillus subtilis*, possessing a strong antifungal activity against *Fusarium solani**

Weixiang LIU[1, 2], Chaomin SUN[1, 2, **]

[1] *CAS and Shandong Province Key Laboratory of Experimental Marine Biology*, *Institute of Oceanology*, *Center for Ocean Mega-Science*, *Chinese Academy of Sciences*, *Qingdao 266071*, *China*

[2] *Laboratory for Marine Biology and Biotechnology*, *Pilot National Laboratory for Marine Science and Technology* (*Qingdao*), *Qingdao 266237*, *China*

Received Jun. 2, 2020; accepted in principle Sep. 22, 2020; accepted for publication Oct. 8, 2020

Abstract Root rot disease caused by *Fusarium solani* is the most devastating disease of the tomato and legume crops in China. The metabolites of *Bacillus* species can inhibit many fungal diseases. In this study, the metabolites of deep-sea-derived bacterium *Bacillus subtilis* 2H11 can significantly inhibit the growth of *F. solani*. The metabolite C_{17}-fengycin B, one of the cyclic lipopeptides, was identified by the combination of silica column chromatography, high-performance liquid chromatography (HPLC), high-energy collision induced dissociation mass spectrometry (HCD-MS) and tandem mass spectrometry (HCD-MS/MS). The results of scanning electron microscopy (SEM) and transmission electron microscopy (TEM) showed that C_{17}-fengycin B could destroy the structure of the hyphae and spores of *F. solani*. The antifungal activities of C_{17}-fengycin B against *F. solani* were tested at concentrations ranging from 0.05 mg/mL to 0.20 mg/mL. The results indicated that C_{17}-fengycin B inhibited the growth of *F. solani* with antifungal index of 89.80% at 0.20 mg/mL, and the antifungal activity of C_{17}-fengycin B was further verified by the pot experiment. In addition, the cytotoxicity experiment showed that C_{17}-fengycin B had good biocompatibility and was a potential candidate for the development of biocontrol pesticide in the future.

Keyword: *Bacillus* species; lipopeptide; fengycin; antifungal; pesticide

1 INTRODUCTION

Root rot is a kind of soil-borne disease which is common in the global economic crop production area (Egamberdieva et al., 2017). The first research on root rot was reported by von Schrenk in 1902 when he was studying apple tree diseases (Von Schrenk and Spaulding, 1902). Since then, root rot infections have been found in potato (Al-Mughrabi et al., 2013), soybean (Cui et al., 2016), cucumber (Wiggell and Simpson, 1969) and other crops. At present, root rot has become one of the main diseases of economic crops, which can reduce the yield by 25%–60% in serious cases (Coetzee et al., 2018). Root rot can be caused by a variety of soil microorganisms, among which *Fusarium* spp. is the main group (Egamberdieva et al., 2017; Chang et al., 2018). *Fusarium* spp. has a wide range of distribution, and *Fusarium solani* is the main pathogen of root rot because of its high isolation frequency and strong pathogenicity (Chittem et al., 2015; Schroers et al., 2016). At present, the control strategies of *Fusarium* mainly include chemical control and biological control (Patzke et al., 2017; D'Agostino et al., 2018). Among them, chemical control method has the advantages of low cost, good effect, quick effect and easy to use, which has been wildly used (Bonilla-Landa et al., 2018). However, excessive use of chemical

* Supported by the National Key R&D Program of China (No. 2018YFC0310800), the China Ocean Mineral Resources R&D Association Grant (No. DY135-B2-14), the Strategic Priority Research Program of the Chinese Academy of Sciences (No. XDA22050301), the Taishan Young Scholar Program of Shandong Province (No. tsqn20161051), the Qingdao Innovation Leadership Program (No. 18-1-2-7-zhc) for Chaomin SUN, and the China Postdoctoral Science Foundation (No. 2019M652492)
** Corresponding author: sunchaomin@qdio.ac.cn

pesticides will lead to soil pollution, food pesticide residues, and other problems, which brings a huge threat to environment and food safety (Lewis et al., 2016; Shugart, 2017; Nile et al., 2019). At the same time, long-term use of chemical pesticides will lead to drug resistance of pathogenic microorganisms (Sav et al., 2018; da Rosa et al., 2019). Therefore, it is an urgent task to find new effective and green biological pesticides to control root rot (Azizbekyan, 2019).

For decades, researchers have been studying marine natural products and found a series of compounds with significant biological activities (Blunt et al., 2018). Marine bacteria are an important branch of natural product research. It can be cultured by large-scale fermentation, which solves the problem of limited production of separated compounds and the sustainability of marine microbial resources (Kobayashi, 2016). In 2018 alone, 1 554 new marine derived compounds were reported, many of which have antibacterial, insecticidal, or antitumor activities (Carroll et al., 2020).

Bacillus is a kind of Gram-positive bacteria, which can adapt to a variety of extreme environments, even in the deep sea (Shafi et al., 2017). Research on the secondary metabolites of *Bacillus* from marine environment has been always a hot spot in the research of natural products (Zeigler and Nicholson, 2017). Many types of compounds, such as ester peptide, polypeptide, polyketone, and fatty acid, have been isolated from their metabolites. Meanwhile, these compounds also have antibacterial, antitumor, and other biological activities (Li et al., 2011; Xing et al., 2018). In this study, we purified C_{17}-fengycin B from the metabolites of *B. subtilis* 2H11 (BS2H11) isolated from the sediment of deep-sea cold seep. The structure was analyzed by electrospray ionization mass spectrometry (ESI-MS) and tandem mass spectrometry (ESI-MS/MS). The antifungal property of C_{17}-fengycin B against *F. solani* was evaluated. In addition, we also studied the effects of C_{17}-fengycin B on spores and hyphae of *F. solani* by electron microscopy. The ester peptide derivative may be developed as an agricultural antifungal agent.

2 MATERIAL AND METHOD

2.1 Isolation, identification, and culture conditions of bacterial strains

Marine sediment was collected by RV *Kexue* (*Science* in Chinese) from the cold seep in the South China Sea (119°17′04.956″E, 22°06′58.384″N) at a depth of approximately 1 143 m in September 2017. The marine bacterial strain used in this study was isolated from the above-described samples by dilution method and cultured in the improved ZoBell 2216E broth (5-g/L tryptone, 1-g/L yeast extract, 1-L filtered seawater, pH adjusted to 7.4 to 7.6), with the temperature of 28 °C (Schut et al., 1993). To determine the phylogenetic position of the bacterial strain, universal primers 27F (5′-AGAGTTTGATCCTGG-CTCAG-3′) and 1492R (5′-TACGGCTACCTTGT-TACGACTT-3′) specific for bacterial 16S rRNA genes were used to amplify the corresponding gene. Then, NCBI-BLAST (see http://www.ncbi.nlm.nih.gov/BLAST) and the phylogenetic analysis program MEGA6 were used to compare the 16S rRNA gene sequence with related sequence in public databases (Tamura et al., 2013).

2.2 Screening of bacteria inhibiting the growth of *F. solani*

In this study, *F. solani*, the main pathogen of root rot, was taken as the target fungus. To determine the antifungal activity of the bacteria strain, the surface plating method was used. The test method was as previously described in Zhang and Sun (2018). The bacterial suspension was incubated overnight and adjusted to 0.2 at 600 nm (OD_{600}). *F. solani* was placed on potato glucose agar (PDA) plate and cultured at 28 °C for 5 d. The hyphal plug (0.5 cm in diameter) removed from the edge of the *F. solani* culture was placed in the center of the new plate. Ten microliters of different bacteria were inoculated 3 cm from the plug edge of *F. solani*. Plates containing only *F. solani*, or plates containing different bacteria and *F. solani*, were incubated at 28 °C for another 3 days, and then the growth area of fungi was measured. Then, the results were obtained by observing the presence (growth) or absence (non-growth) of fungi.

2.3 Isolation, purification, and identification of antifungal compound from *B. subtilis* 2H11

The single colony of *B. subtilis* 2H11 strain was inoculated into a 250-mL flask containing 100-mL of Luria-Bertani (LB) medium and cultured at 180 r/min for 24 h at 28 °C. Then 10 mL of this seed culture was inoculated into a 3-L flask containing 1 L of LB medium and cultured at 180 r/min for another 24 h at 28 °C. The supernatant was obtained by centrifuging the fermentation broth (8 000×*g*, 4 °C, 10 min). The pH of the supernatant was adjusted to 2.5 with 6 mol/L HCl at 4 ℃. When the solution turned clear, the precipitate was obtained by centrifugation (8 000×*g*,

4 °C, 10 min), washed with 0.1 mol/L HCl and then extracted with methanol filtered through a 0.22-μm membrane and concentrated under reduced pressure. The supernatant was then passed through a Sephadex LH-20 column for fractionation and eluted with methanol as the mobile phase (Ramos and Prohaska, 1981). The eluted fraction was concentrated with a vacuum rotary evaporator and determined for antifungal activity using the paper disc method (Kordali et al., 2008). The eluted fraction with antifungal activity was filtered through a 0.22-μm membrane filter and further purified by reversed-phase high performance liquid chromatography (RP-HPLC) (Agilent 1260) equipped with an Eclipse XDB-C18 column (5 μm, 9.4×250 mm). The mobile phase A consisting of water and methanol (20∶80, v/v) and the mobile phase B was methanol. The eluting strategy was as follows: 0–20 min, 0% B; 20–60 min, 0% B to 100% B and 60–80 min, 100% B. The flow rate was 2 mL/min and the elution was monitored using a UV detector set at 210 nm. Each elution peak was collected and the antifungal activity was determined. The stability of the active compound(s) was determined by HPLC column twice.

Mass spectra of active antifungal substances was analyzed by linear ion trap Orbitrap spectrometer (LTQ Orbitrap XL, Thermo fisher) using high-energy collision induced dissociation (HCD), which was a new mass spectrometry pyrolysis technology and could provide abundant fragmentation information. Data from HCD-MS/MS were acquired under the following conditions: electrospray ion source (ESI), spray voltage 3 kV, ion transfer capillary temperature 275 °C; the dry gas was nitrogen gas, and the pressure was 0.05 MPa; HCD collision gas was helium, anion pattern detection; the collision energy of HCD is 45–60 eV. And then the results were analyzed by Xcalibur 2.1 (Thermo Fisher Scientific Inc, Waltham, MA).

2.4 Antifungal assay (in vitro)

The antifungal activity was evaluated in-vitro against *F. solani* by a mycelium growth rate test. Data were collected as previously described in literature (de Rodríguez et al., 2005). The antifungal activity was detected at the concentrations of 0.05, 0.10, and 0.20 mg/mL, respectively. The plates inoculated with mycelia of *F. solani* was cultured at 27 °C. When the mycelium reached the edge of the negative control plate (no sample was added), the antifungal index was calculated by the following formula:

Antifungal index (%)=$(1–D_a/D_b)\times100$.

D_a and D_b are the diameter of hyphae in the test plate and negative control plate respectively. Each test was repeated three times, and the results were averaged.

2.5 Protective and curative Activity (in vivo)

In this study, in-vivo antifungal activity was measured by pot experiment, and the protective and curative activity of the samples were measured. Because of the large amount of samples needed in the pot experiment, the crude extract was used. Data were collected as previously described in Benaouali et al. (2014). The experiment was carried out when tomato seedlings were cultured to at least 8 true leaves. For protective activity, the seedlings were treated with 10-mL test reagents of 0.40 and 0.80 mg/mL, respectively. 24 hours later, the spore suspension was adjusted to 3.5×10^3 spores/mL, and 2 mL of spore suspension was used to irrigate the seedlings. For curative activity, the sample treatment and spore suspension treatment time were exchanged. Tomato seedlings were treated with spore suspension at first, and then treated with sample after 24 h. Then the seedlings were cultured at 25±3 °C and 85% humidity. Each treatment was repeated in 3 groups. Seven days later, the disease index and control efficacy were calculated.

2.6 Morphology changes of *F. solani* hyphae following C_{17}-fengycin B treatment

Scanning electron microscope (SEM) was used to determine the effects of C_{17}-fengycin B on hyphae of *F. solani* at the ultrastructural level. C_{17}-fengycin B was spotted on a small sterilized filter paper and placed 2 cm away from the edge of the margin of freshly grown *F. solani*. The hyphae with or without C_{17}-fengycin B treatment was prefixed with 2.5% glutaraldehyde. Fixed cells were rinsed three times for 10 min with 10 mmol/L Phosphate buffer solution (PBS) (pH 7.2 to 7.4). The samples were dehydrated through an ethanol gradient and coated with gold. Hitachi S-3400N scanning electron microscope was used for analysis (Hitachi, Tokyo, Japan).

2.7 Morphology changes of *F. solani* spores following C_{17}-fengycin B treatment

To induce the formation of sporangium, six hyphal plugs were cut from a 1–2 week culture dish, covered with sterile distilled water and placed in a growth chamber for 48 h at 25 °C, and the light intensity was

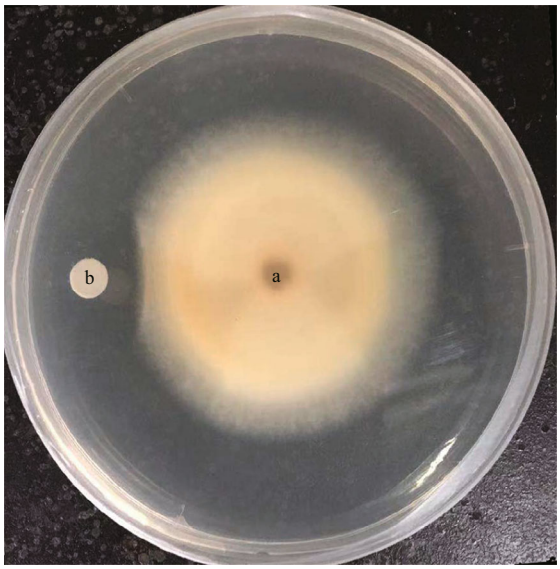

Fig.1 Antifungal assay of *B. subtilis* 2H11 (b) against *F. solani* (a)

1 400 lx (Matheron and Porchas, 2000). Then the culture dish was placed at 4 °C for 1 h to promote the release of spores. The spores were washed with distilled water and the concentration of spores was checked under microscope. After spores were collected, C_{17}-fengycin B was added into spore suspension (1×10^5 spores/mL) of equal volume. The final concentration was 0, 0.10, and 0.20 mg/mL, respectively. The spores were incubated at 25 °C in dark for 1 h. The germination of spores was examined by transmission electron microscopy. The germination of spores was examined by transmission electron microscopy (TEM) (HT7700 Hitachi).

2.8 Cytotoxicity assay

In-vitro cytotoxicity of C_{17}-fengycin B on LO2 cell line was evaluated by methyl thiazolyl tetrazolium (MTT) assay (Hu et al., 2014). LO2 cells (1×10^5 cells/well) were inoculated in 96-well flat-bottom culture plate and cultured in incubator for 24 h, and then introduced C_{17}-fengycin B, the concentrations were 0.05, 0.10, and 0.20 mg/mL, individually. 24 hours later, the supernatants were removed, and 100-μL MTT working solution were added into each well. After incubation for 4 h, the formazan crystals were dissolved by MTT stopping buffer for 18 h and determined spectrophotometrically at 550 nm by a microplate reader (Infinite M1000 Pro, TECAN, Mannedorf, Switzerland).

2.9 Statistical analysis

Repeat each test three times and take the average result. All the data were expressed by the mean±SD of four independent measurements, and ANOVA was performed by SPSS software (version 18.0 for windows, SPSS, Inc., Chicago, IL, USA). The mean comparison was performed by Duncan's multiple comparison test. Statistical differences were significant at $P<0.05$.

2.10 Accession number

The GenBank accession number for the 16S rRNA gene of *B. subtilis* 2H11 is MT211278.

3 RESULT AND DISCUSSION

3.1 Antifungal activity of marine bacterium *B. subtilis* 2H11 against *F. solani*

In this study, more than 100 marine cold seep bacteria were screened through antagonistic experiments, and their ability to inhibit the growth of *F. solani* was evaluated in an order to obtain metabolites with antifungal activity. According to the plate assays, strain 2H11 was proved to significantly inhibit the growth of *F. solani* (Fig.1). In addition, the expansion of the edge of *F. solani* colony was inhibited even when *B. subtilis* 2H11 was not contacted, which indicated that the metabolites produced by *B. subtilis* 2H11 could inhibit the growth of *F. solani* hyphae. By comparing the 16S rRNA sequence with relevant sequences in NCBI website, it was found that the strain had the highest homology with *B. subtilis* strain JCM1465 (Supplementary Fig. S1), and the sequence similarity reached 99%. Therefore, the marine bacterial strain 2H11 was designated as *B. subtilis* 2H11.

3.2 Isolation, purification, and identification of antifungal compounds from *B. subtilis* 2H11

To obtain compound(s) with antifungal activity from *B. subtilis* 2H11, purification was performed as described in the Materials and Methods. Using *F. solani* as the indicator fungus, the paper disc method was used to trace the bioactive compound(s). In the RP-HPLC chromatogram (Fig.2a), we found a single peak related to antifungal activity, indicating that the compound here has inhibitory effect on the growth of *F. solani*. Then we tested the activity of the compound obtained by RP-HPLC by the filter paper disk test, and found that they had strong antifungal activity against *F. solani* (Fig.2b). The chemical structure of the compound was further analyzed and

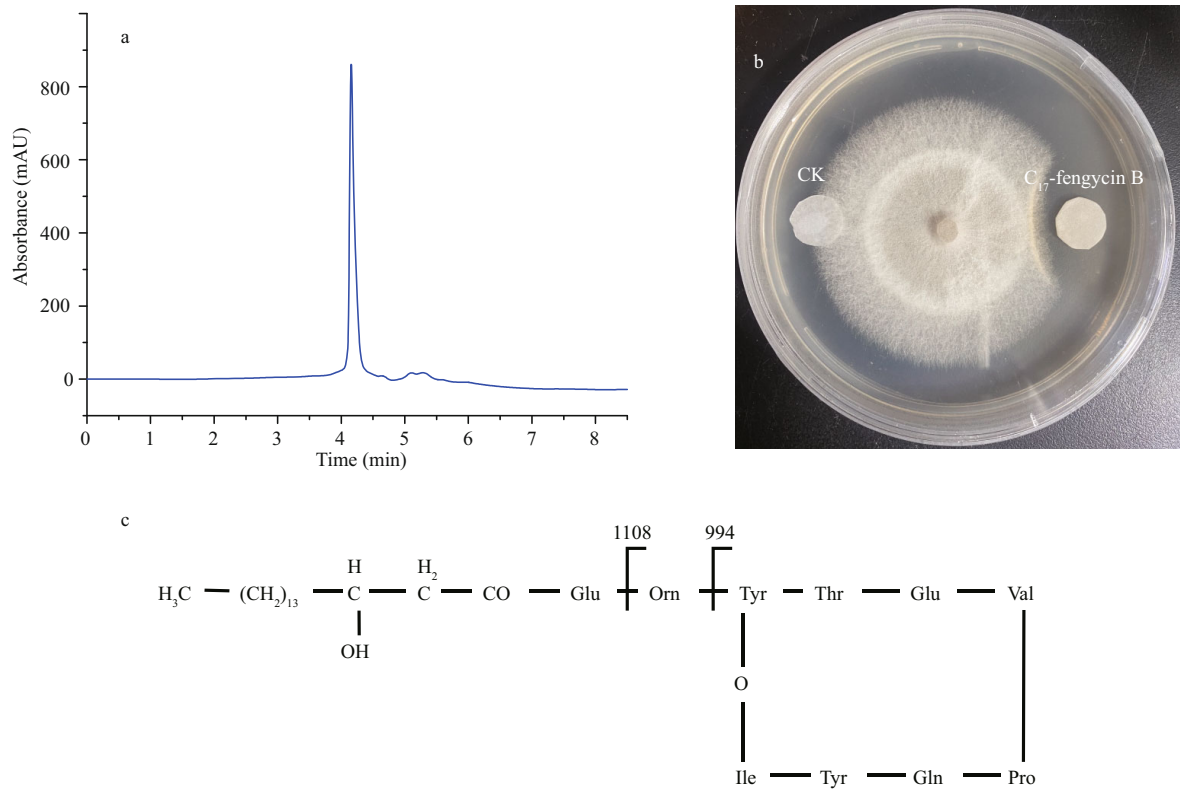

Fig.2 Purification and characterization of the active compounds from *B. subtilis* 2H11 inhibiting the growth of *F. solani*

a. HPLC analysis of the active component from *B. subtilis* 2H11; b. the inhibitory effect of the active compound from *B. subtilis* 2H11 on the growth of *F. solani* mycelia; c. chemical structures and fragmentation patterns of C_{17}-fengycin B, which was isolated from *B. subtilis* 2H11 as the active compound.

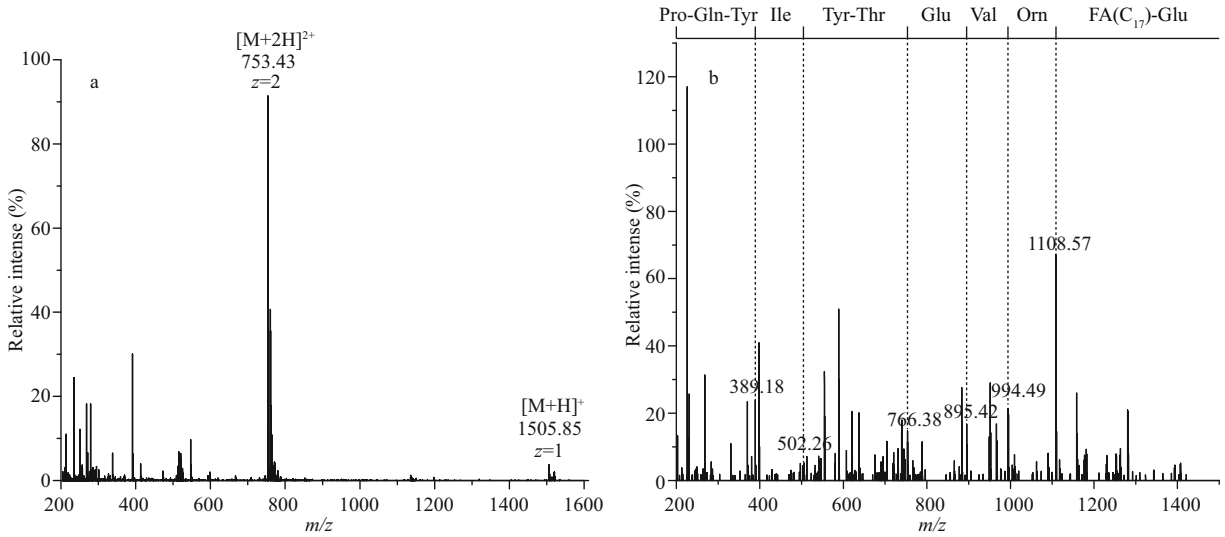

Fig.3 Structure elucidation of C_{17}-fengycin B by HCD-MS (a) and HCD-MS/MS (b)

elucidated by mass spectrometry.

In the results of HCD-MS and HCD-MS/MS, we found the singly- and doubly-protonated molecular ions at *m/z* 1 505.85 $[M+H]^+$ and *m/z* 753.43 $[M+2H]^{2+}$, respectively (Fig.3a). Therefore, the molecular weight of the purified active compound was 1 505 Da. It should be noted that the result is consistent with the MS data of fengycin cyclic lipopeptide (CLP) previously reported (Zhang and Sun, 2018). The typical fragmentation ions *m/z* 994 and 1 108 in the secondary mass spectrometry were caused by the loss of fatty acid-Glu (-398 Da) and fatty acid-Glu-Orn (-512 Da) from the N-terminal segment with a Val residue at position 6 in C_{17}-

Table 1 Protective and curative activities of C_{17}-fengycin B against *F. solani*

Sample	Concentration (mg/mL)	Protective activity		Curative activity	
		Disease index	Control efficacy (%)	Disease index	Control efficacy (%)
C_{17}-fengycin B	0.4	27.78±12.73^{ab}	64.07±17.44^{a}	33.33±14.43^{a}	59.66±18.32^{a}
	0.8	11.11±9.62^{a}	85.19±12.83^{a}	22.22±4.81^{a}	73.50±3.95^{a}
Polymyxin B	0.4	33.33±14.43^{b}	57.41±17.86^{a}	27.78±20.97^{a}	67.20±24.91^{a}
	0.8	16.67±8.33^{ab}	78.52±11.18^{a}	16.67±14.43^{a}	79.93±17.29^{a}
H_2O	–	77.78±4.81^{c}	–	83.33±8.33^{b}	–

– means no data. $^{a, b}$ represent the levels of significant difference which were obtained according to Duncan's test.

fengycin B cyclic decapeptide, respectively (Fig.3b) (Chen et al., 2010; Pecci et al., 2010). The loss of fatty acid-Glu and fatty acid-Glu-Orn usually results in the simultaneous emergence of nine peptide (Orn-Tyr-Thr-Glu-Val-Pro-Glu-Tyr-Ile, *m/z* 1 108) and octapeptide (Tyr-Thr-Glu-Val-Pro-Glu-Tyr-Ile, *m/z* 994) as integral fragmentation ions. In conclusion, HCD-MS and HCD-MS/MS spectral data are consistent with the corresponding information of C_{17}-fengycin B (Fig.2c) (Pecci et al., 2010). Therefore, the antifungal metabolite produced by *B. subtilis* 2H11 was demonstrated as C_{17}-fengycin B.

3.3 In-vitro antifungal activity of the purified C_{17}-fengycin B against *F. solani*

The secondary metabolites of marine-derived *Bacillus* have been one of the hotspots in natural products research. Many kinds of compounds have been isolated from their metabolites. Among them, fengycin CLPs have attracted much attention due to their antifungal (Chen et al., 2010; Ma et al., 2014; Nam et al., 2015). In this essay, *F. solani*, the pathogenic fungus of root rot, was selected as the target. C_{17}-fengycin B was dissolved in dimethyl sulfoxide (DMSO). The original concentration was 0.80 mg/mL. The antifungal results of C_{17}-fengycin B are shown in Fig.4. The inhibitory effects of C_{17}-fengycin B were compared with those of polymyxin B that is a polypeptide antibiotic and has a strong inhibitory effect on a variety of microorganisms. It has been widely used in many fields, and is a typical lipopeptide antibiotic. Therefore, we set it as the positive control to facilitate comparative analysis.

It was observed that C_{17}-fengycin B exhibited relatively high inhibitory effect against *F. solani*, and the inhibitory rates were 65.10%, 71.37%, and 89.80% at the concentrations of 0.05, 0.10, and 0.20 mg/mL, respectively. At the same doses, the inhibition rate of positive control polymyxin B was slightly higher than those of C_{17}-fengycin B, and

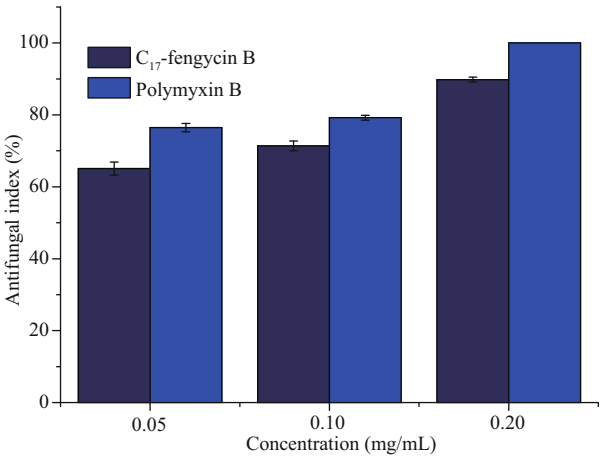

Fig.4 Antifungal activity of C_{17}-fengycin B and polymyxin B against *F. solani*

polymyxin B could inhibit the growth of *F. solani* 100% at 0.20 mg/mL. Some studies have shown that there is a certain relationship between the antifungal activity of lipopeptide antibiotics and their hydrophobicity (Thiericke and Rohr, 1993). Generally, in the RP-HPLC system, the elution time has a positive relationship with the hydrophobicity of molecules, that is, the longer the elution time, the stronger the hydrophobicity performance. Therefore, we conclude that hydrophobic groups in C_{17}-fengycin B may play an important role for the antifungal activity.

3.4 In-vivo protective and curative activities of C_{17}-fengycin B

The protective and curative activities of C_{17}-fengycin B are shown in Table 1 and Supplementary Fig.S2. The disease indexes of tomato irrigated with C_{17}-fengycin B were significantly lower than that of the negative control group irrigated with water. In addition, the control efficacy of C_{17}-fengycin B increased with its concentrations. At the concentration of 0.8 mg/mL, the protective activity and curative activity of C_{17}-fengycin B were 85.19% and 73.50%,

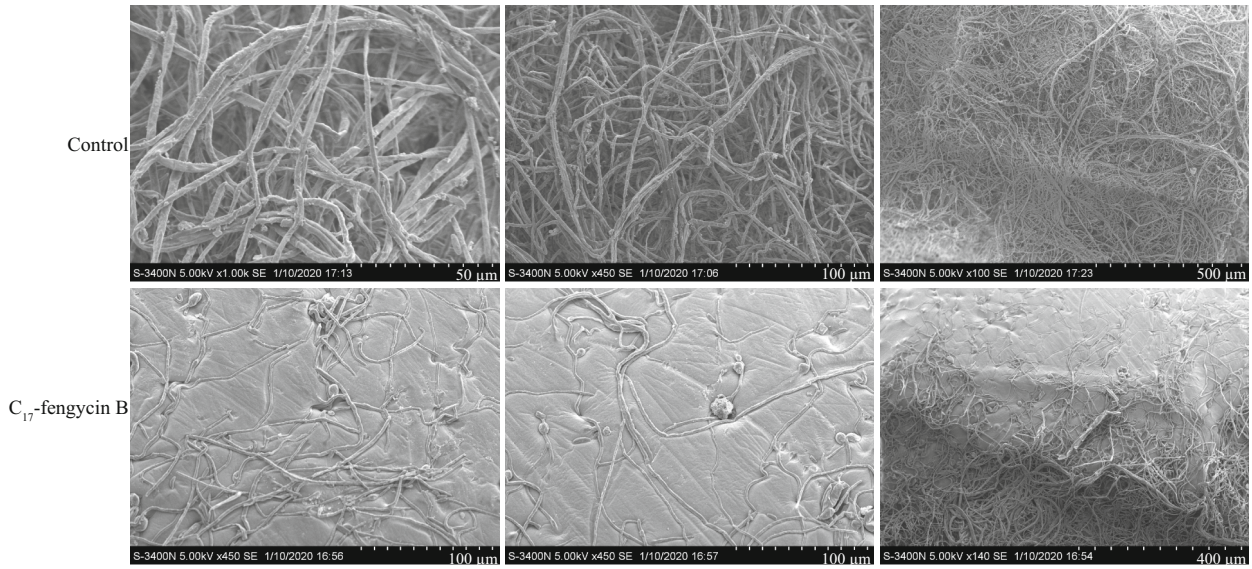

Fig.5 Effects of C_{17}-fengycin B on the morphology of *F. solani* hyphae observed by SEM

In the control groups, *F. solani* hyphal cells were treated with methanol (0.04% [v/v]). In the test groups, *F. solani* hyphal cells were treated with 0.05 mg/mL C_{17}-fengycin B.

respectively, which were close to those of positive control polymyxin B. There were no obvious pathological changes in the roots of seedlings treated with C_{17}-fengycin B, and the roots were not blackened. Moreover, in contrast to the positive control polymyxin B, the protective activity of C_{17}-fengycin B was higher than that of its curative activity at the same concentration, which indicated that the antifungal activity of C_{17}-fengycin B would not be damaged by the soil and would play a sustainable role in the application.

3.5 Morphology changes of *F. solani* hyphae caused by C_{17}-fengycin B

To study the effects of C_{17}-fengycin B on the morphology of *F. solani* hyphae, SEM observation was conducted. As shown in Fig.5, the hyphae of *F. solani* in the control group grew normally, with plump and intact trunks. In contrast, the morphology of hyphae treated with C_{17}-fengycin B was significantly different with the control. Compared with the control group, the amount of hyphae treated with C_{17}-fengycin B was significantly reduced, and the hyphae appeared rough and shriveled.

3.6 Morphology changes of *F. solani* spores caused by C_{17}-fengycin B

TEM was used to observe the effects of C_{17}-fengycin B on the morphology changes of *F. solani* spores (Fig.6). The normal fungal spores have intact and regular cell walls and membranes, with dense cytoplasm and uniform spatial distribution in the intracellular space. However, after C_{17}-fengycin B treatment, the cytoplasm became sparse and light, and the cell membrane became incomplete or even ruptured. At the same time, we also found that higher concentration of C_{17}-fengycin B destroyed spores more seriously, which indicated that the antifungal activity of C_{17}-fengycin B was positively correlated with its concentration. In conclusion, the electron microscopy results showed that C_{17}-fengycin B can damage the cytoplasm and membrane of *F. solani* and destroy the integrity of cells.

3.7 Cytotoxicity assay

As we all know, most chemical fungicides have strong toxicity. These fungicides are harmful to insects, animals, and human beings. Therefore, the search for new fungicides with low toxicity and high efficiency has always been an important field of pesticide research. At present, most of the studies on the cytotoxicity of fengycin CLPs focus on their antitumor activity, but few on the cytotoxicity of normal animal cells (Yin et al., 2013; Ramachandran et al., 2017; Rofeal and El-Malek, 2020). The results showed that some fengycin CLPs had significant cytotoxicity to human embryonic kidney 293 (HEK293), human internalized keratinocyte (HaCaT), human cervical cancer (Hela), and human type II alveolar epithelial (A549) cell lines. In this study, we used LO2 cells as the target to test the cytotoxicity of C_{17}-fengycin B. The effects are listed in Fig.7, showing

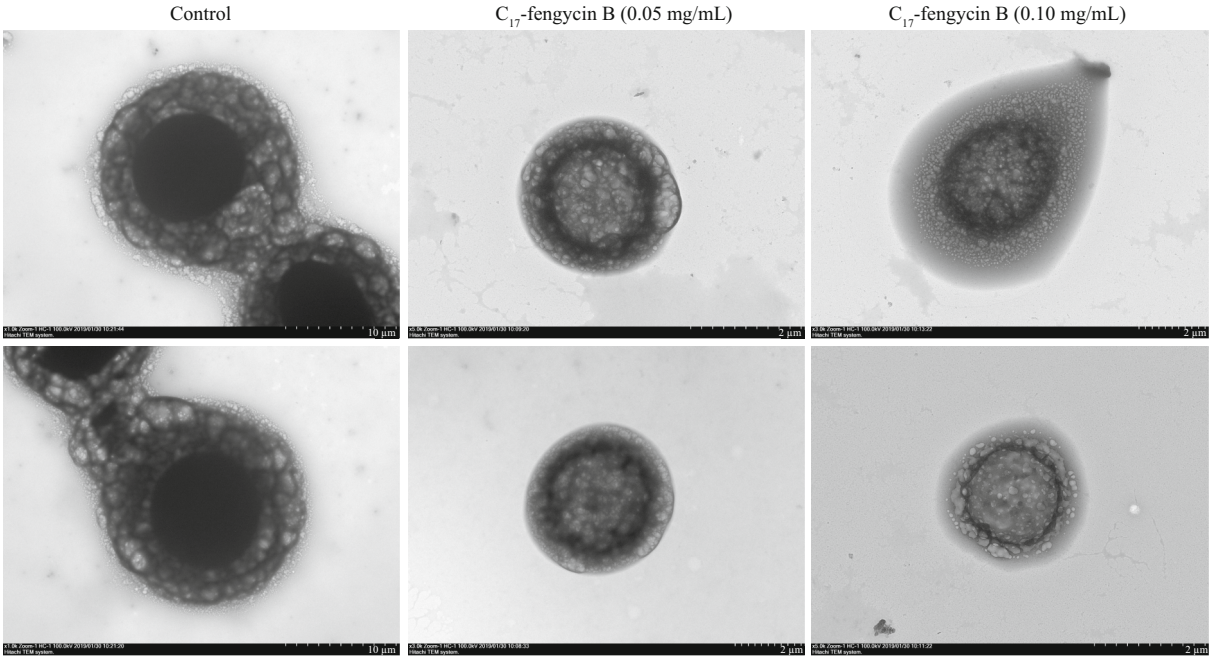

Fig.6 Effects of C_{17}-fengycin B on the morphology of *F. solani* spores observed by TEM

In the control groups, *F. solani* spores were treated with methanol (0.04% [v/v]). In the test groups, *F. solani* spores were treated with 0.05 mg/mL and 0.10 mg/mL C_{17}-fengycin B, respectively.

that at the concentrations of 0.05 and 0.10 mg/mL, the cell viability of LO2 cells treated with C_{17}-fengycin B was 91.54% and 83.46%, respectively. In addition, at the same concentration, the cytotoxicity of C_{17}-fengycin B was significantly lower than that of positive control polymyxin B. These results indicate that C_{17}-fengycin B has good biocompatibility to LO2 cells and has the potential to develop into an environmental friendly biological fungicide.

In this study, the presence of C_{17}-fengycin B (0.05 mg/mL) appeared to have no effect on LO2 cells. Compared with chemical method, microbial fermentation has the advantages of low cost, environment-friendly, and easily scaled up for large scale synthesis. This study demonstrated that C_{17}-fengycin B can be used as a biofungicide to control root rot caused by *F. solani*. C_{17}-fengycin B showed strong antifungal activity in vitro and in vivo, and had a low cytotoxicity to LO2 cells.

The results can provide a new idea for the control of root rot in the future. The biosynthesis of C_{17}-fengycin B by *B. subtilis* is an efficient, green, and sustainable method. This will greatly reduce the environmental pollution and pesticide residues caused by chemical pesticide production. However, before developing the agricultural application of C_{17}-fengycin B, it is necessary to do more researches on the antifungal mechanism of C_{17}-fengycin B.

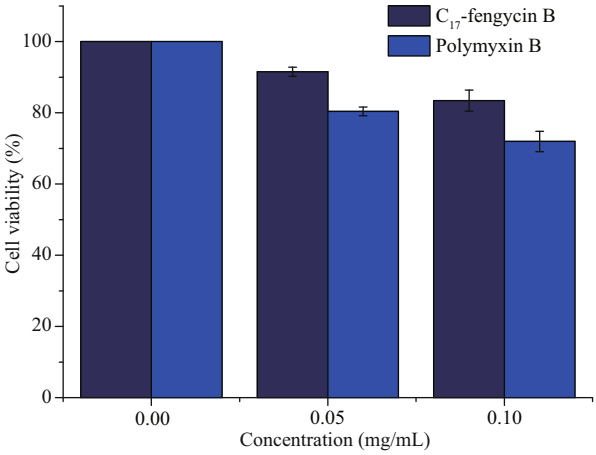

Fig.7 The toxicity of C_{17}-fengycin B on LO2 cells

4 CONCLUSION

This study was conducted to determine the activity of cyclic lipopeptide C_{17}-fengycin B, produced by deep-sea bacterium *B. subtilis* 2H11, in the suppression of *F. solani* (pathogen of the tomato root rot disease). The structure of C_{17}-fengycin B was confirmed by HCD-MS and HCD-MS/MS. The antifungal effects of C_{17}-fengycin B against *F. solani* was evaluated in-vitro and in-vivo. The results show that C_{17}-fengycin B could effectively inhibit the growth of *F. solani*. At the same dose, the inhibition rate of C_{17}-fengycin B was slightly lower than that of positive control polymyxin B. In addition, a cytotoxicity assay of C_{17}-

fengycin B was also performed, and the results show that the cytotoxicity of C_{17}-fengycin B was significantly lower than that of polymyxin B. Moreover, the hyphae and spores of *F. solani* treated with C_{17}-fengycin B were observed by electron microscope, and the antifungal mechanism of C_{17}-fengycin B was discussed. In conclusion, C_{17}-fengycin B has a good antifungal activity and biocompatibility, it could be a potential candidate for the development of biocontrol pesticide.

5 DATA AVAILABILITY STATEMENT

The data that support the findings are all presented herein.

References

Al-Mughrabi K I, Vikram A, Peters R D, Howard R J, Grant L, Barasubiye T, Lynch K, Poirier R, Drake K A, Macdonald I K, Lisowski S L I, Jayasuriya K E. 2013. Efficacy of *Pseudomonas syringae* in the management of potato tuber diseases in storage. *Biological Control*, **64**(3): 315-322.

Azizbekyan R R. 2019. Biological preparations for the protection of agricultural plants (Review). *Applied Biochemistry and Microbiology*, **55**(8): 816-823.

Benaouali H, Hamini-Kadar N, Bouras A, Benichou S L, Kihal M, Henni J E. 2014. Isolation, pathogenicity test and physicochemical studies of *Fusarium oxysporum* f.sp radicis lycopersici. *Advances in Environmental Biology*, **8**(10): 36-49.

Blunt J W, Carroll A R, Copp B R, Davis R A, Keyzers R A, Prinsep M R. 2018. Marine natural products. *Natural Product Reports*, **35**(1): 8-53.

Bonilla-Landa I, de la Cruz O L, Sanchéz-Rangel D, Ortíz-Castro R, Rodriguez-Haas B, Barrera-Méndez F, de León Gómez R E D, Javier Enríquez-Medrano F, Luis Olivares-Romero J. 2018. Design, synthesis and biological evaluation of novel fungicides for the management of *Fusarium DieBack* disease. *Journal of the Mexican Chemical Society*, **62**(3): 86-98.

Carroll A R, Copp B R, Davis R A, Keyzers R A, Prinsep M R. 2020. Marine natural products. *Natural Product Reports*, **37**(2): 175-223.

Chang X L, Dai H, Wang D P, Zhou H H, He W Q, Fu Y, Ibrahim F, Zhou Y, Gong G S, Shang J, Yang J Z, Wu X L, Yong T W, Song C, Yang W Y. 2018. Identification of *Fusarium* species associated with soybean root rot in Sichuan Province, China. *European Journal of Plant Pathology*, **151**(3): 563-577.

Chen L L, Wang N, Wang X M, Hu J C, Wang S J. 2010. Characterization of two anti-fungal lipopeptides produced by *Bacillus amyloliquefaciens* SH-B10. *Bioresource Technology*, **101**(22): 8 822-8 827.

Chittem K, Mathew F M, Gregoire M, Lamppa R S, Chang Y W, Markell S G, Bradley C A, Barasubiye T, Goswami R S. 2015. Identification and characterization of *Fusarium* spp. associated with root rots of field pea in North Dakota. *European Journal of Plant Pathology*, **143**(4): 641-649.

Coetzee M P A, Wingfield B D, Wingfield M J. 2018. Armillaria root-rot pathogens: species boundaries and global distribution. *Pathogens*, **7**(4): 83, https://doi.org/10.3390/pathogens7040083.

Cui J Q, Wang Y, Han J, Cai B Y. 2016. Analyses of the community compositions of root rot pathogenic fungi in the soybean rhizosphere soil. *Chilean Journal of Agricultural Research*, **76**(2): 179-187.

da Rosa P D, Ramirez-Castrillon M, Borges R, Aquino V, Fuentefria A M, Goldani L Z. 2019. Epidemiological aspects and characterization of the resistance profile of *Fusarium* spp. in patients with invasive fusariosis. *Journal of Medical Microbiology*, **68**(10): 1 489-1 496.

D'Agostino M, Lemmet T, Dufay C, Luc A, Frippiat J P, Machouart M, Debourgogne A. 2018. Overinduction of CYP51A gene after exposure to azole antifungals provides a first clue to resistance mechanism in *Fusarium solani* species complex. *Microbial Drug Resistance*, **24**(6): 768-773.

de Rodríguez D J, Hernández-Castillo D, Rodríguez-García R, Angulo-Sánchez J L. 2005. Antifungal activity in vitro of *Aloe vera* pulp and liquid fraction against plant pathogenic fungi. *Industrial Crops and Products*, **21**(1): 81-87.

Egamberdieva D, Wirth S J, Shurigin V V, Hashem A, Abd Allah E F. 2017. Endophytic bacteria improve plant growth, symbiotic performance of chickpea (*Cicer arietinum* L.) and induce suppression of root rot caused by *Fusarium solani* under salt stress. *Frontiers in Microbiology*, **8**: 1 887, https://doi.org/10.3389/fmicb.2017.01887.

Hu W C, Wang G C, Li P X, Wang Y N, Si C L, He J, Long W, Bai Y J, Feng Z S, Wang X F. 2014. Neuroprotective effects of macranthoin G from *Eucommia ulmoides* against hydrogen peroxide-induced apoptosis in PC12 cells via inhibiting NF-κB activation. *Chemico-Biological Interactions*, **224**: 108-116.

Kobayashi J I. 2016. Search for new bioactive marine natural products and application to drug development. *Chemical & Pharmaceutical Bulletin*, **64**(8): 1 079-1 083.

Kordali S, Cakir A, Ozer H, Cakmakci R, Kesdek M, Mete E. 2008. Antifungal, phytotoxic and insecticidal properties of essential oil isolated from Turkish *Origanum acutidens* and its three components, carvacrol, thymol and *p*-cymene. *Bioresource Technology*, **99**(18): 8 788-8 795.

Lewis K A, Tzilivakis J, Warner D J, Green A. 2016. An international database for pesticide risk assessments and management. *Human and Ecological Risk Assessment*: *an International Journal*, **22**(4): 1 050-1 064.

Li D H, Carr G, Zhang Y H, Williams D E, Amlani A, Bottriell H, Mui A L F, Andersen R J. 2011. Turnagainolides A and B, cyclic depsipeptides produced in culture by a *Bacillus* sp.: Isolation, structure elucidation, and synthesis. *Journal of Natural Products*, **74**(5): 1 093-1 099.

Ma Z W, Hu J C, Wang X M, Wang S J. 2014. NMR spectroscopic and MS/MS spectrometric characterization

of a new lipopeptide antibiotic bacillopeptin B1 produced by a marine sediment-derived *Bacillus amyloliquefaciens* SH-B74. *The Journal of Antibiotics*, **67**(2): 175-178.

Matheron M E, Porchas M. 2000. Impact of azoxystrobin, dimethomorph, fluazinam, fosetyl-Al, and metalaxyl on growth, sporulation, and zoospore cyst germination of three *Phytophthora* spp. *Plant Disease*, **84**(4): 454-458.

Nam J, Jung M Y, Kim P I, Lee H B, Kim S W, Lee C W. 2015. Structural characterization and temperature-dependent production of C_{17}-fengycin B derived from *Bacillus amyloliquefaciens* subsp. plantarum BC32-1. *Biotechnology and Bioprocess Engineering*, **20**(4): 708-713.

Nile A S, Kwon Y D, Nile S H. 2019. Horticultural oils: possible alternatives to chemical pesticides and insecticides. *Environmental Science and Pollution Research*, **26**(21): 21 127-21 139.

Patzke H, Zimdars S, Schulze-Kaysers N, Schieber A. 2017. Growth suppression of *Fusarium culmorum*, *Fusarium poae* and *Fusarium graminearum* by 5-*n*-alk(en) ylresorcinols from wheat and rye bran. *Food Research International*, **99**: 821-827.

Pecci Y, Rivardo F, Martinotti M G, Allegrone G. 2010. LC/ESI-MS/MS characterisation of lipopeptide biosurfactants produced by the *Bacillus licheniformis* V9T14 strain. *Journal of Mass Spectrometry*, **45**(7): 772-778.

Ramachandran R, Shrivastava M, Narayanan N N, Thakur R L, Chakrabarti A, Roy U. 2017. Evaluation of antifungal efficacy of three new cyclic lipopeptides of the class bacillomycin from *Bacillus subtilis* RLID 12.1. *Antimicrobial Agents and Chemotherapy*, **62**(1): e01457-17, https://doi.org/10.1128/AAC.01457-17.

Ramos L S, Prohaska P G. 1981. Sephadex LH-20 chromatography of extracts of marine sediment and biological samples for the isolation of polynuclear aromatic hydrocarbons. *Journal of Chromatography A*, **211**(2): 284-289.

Rofeal M, El-Malek A F. 2020. Valorization of lipopeptides biosurfactants as anticancer agents. *International Journal of Peptide Research and Therapeutics*, https://doi.org/10.1007/s10989-020-10105-8.

Sav H, Rafati H, Oz Y, Dalyan-Cilo B, Ener B, Mohammadi F, Ilkit M, van Diepeningen A D, Seyedmousavi S. 2018. Biofilm formation and resistance to fungicides in clinically relevant members of the fungal genus *Fusarium*. *Journal of Fungi* (*Basel*, *Switzerland*), **4**(1): 16, https://doi.org/10.3390/jof4010016.

Schroers H J, Samuels G J, Zhang N, Short D P G, Juba J, Geiser D M. 2016. Epitypification of *Fusisporium* (*Fusarium*) *solani* and its assignment to a common phylogenetic species in the *Fusarium solani* species complex. *Mycologia*, **108**(4): 806-819.

Schut F, De vries E J, Gottschal J C, Robertson B R, Harder W, Prins R A, Button D K. 1993. Isolation of typical marine bacteria by dilution culture: growth, maintenance, and characteristics of isolates under laboratory conditions. *Applied and Environmental Microbiology*, **59**(7): 2 150-2 160.

Shafi J, Tian H, Ji M S. 2017. *Bacillus* species as versatile weapons for plant pathogens: a review. *Biotechnology & Biotechnological Equipment*, **31**(3): 446-459.

Shugart L. 2017. Special Issue: emerging advances and challenges in pesticide ecotoxicology. *Ecotoxicology*, **26**(3): 293-294.

Tamura K, Stecher G, Peterson D, Filipski A, Kumar S. 2013. MEGA6: molecular evolutionary genetics analysis version 6.0. *Molecular Biology and Evolution*, **30**(12): 2 725-2 729.

Thiericke R, Rohr J. 1993. Biological variation of microbial metabolites by precursor-directed biosynthesis. *Natural Product Reports*, **10**(3): 265-289.

Von Schrenk H, Spaulding P. 1902. The bitter rot disease of apples. *Science*, **16**(408): 669-670.

Wiggell P, Simpson C J. 1969. Observations on the control of phomopsis root rot of cucumber. *Plant Pathology*, **18**(2): 71-77, https://doi.org/10.1111/j.1365-3059.1969.tb00469.x.

Xing X Y, Zhao X Y, Ding J, Liu D M, Qi G F. 2018. Enteric-coated insulin microparticles delivered by lipopeptides of iturin and surfactin. *Drug Delivery*, **25**(1): 23-34.

Yin H P, Guo C L, Wang Y, Liu D, Lv Y B, Lv F X, Lu Z X. 2013. Fengycin inhibits the growth of the human lung cancer cell line 95D through reactive oxygen species production and mitochondria-dependent apoptosis. *AntiCancer Drugs*, **24**(6): 587-598.

Zeigler D R, Nicholson W L. 2017. Experimental evolution of *Bacillus subtilis*. *Environmental Microbiology*, **19**(9): 3 415-3 422.

Zhang L, Sun C. 2018. Fengycins, cyclic lipopeptides from marine *Bacillus subtilis* strains, kill the plant-pathogenic fungus *Magnaporthe grisea* by inducing reactive oxygen species production and chromatin condensation. *Applied and Environmental Microbiology*, **84**(18): e00445-18, https://doi.org/10.1128/aem.00445-18.

Electronic supplementary material

Supplementary material (Supplementary Figs.S1–S2) is available in the online version of this article at https://doi.org/10.1007/s00343-020-0215-2.